1
Introduction

The metal solidification process has steadily evolved through ages to grow as a fundamental and yet an awe-inspiring research topic involving rich physics based frame work and essential to a plethora of scientific and engineering application in today's modern era. Although the early evolution of solidification science is mostly experimental and empirical in nature, a fare-share of the present-day research in the field focuses on the development of physics-based numerical models. Modeling and simulations are a cost-effective alternative to time-consuming and expensive experiments. The challenges involving the development of solidification models inclusive of various daunting physical complexities are well worth venturing into, particularly in this modern era endowed with high-performance computation facilities. The knowledge of micro and macro-scale casting defects obtained from numerical simulations apriori allows the relevant industries to refine and upgrade the casting products to a great extent. Therefore, the development of solidification models plays a key role in the present-day advancement of solidification technology. Understanding micro and macro-scale solidification/melting phenomena are of absolute necessity in applications involving conventional casting, semi-solid forming, welding, laser-based surface treatment, atomization, latent heat thermal energy storage, latent heat sink for thermal management of electronic equipment, and many more. Over the last three decades, significant development of solidification models has been attained by several research groups. Both micro and macro-scale modeling received considerable research attention. However, shrinkage or volumetric expansion during solidification, a well-known physical phenomenon that arises due to the difference in densities between solid and liquid phases, is rarely addressed in those models. The present work focuses on including shrinkage or volumetric expansion effects in solidification models at different capacities starting from one-dimensional semi-analytical approach to two and three-dimensional numerical schemes.

1.1 SOLIDIFICATION PROCESS

The process of solidification is an intrinsic mechanism for manufacturing operations involving casting and welding. A cast structure is produced at the end of the solidification process. The mechanical properties of cast products are directly related to the macro and micro-scale morphology and crystal structure, which in turn are governed by the solidification parameters like cooling rate, cooling orientation, initial condition, etc. Often, the desired mechanical properties in a cast product require energy-intensive post-heat-treatment processes. However, the extent of required post-heat-treatment for a cast product can be minimized by controlling suitable parameters at the time of casting itself [Gokhale and Patel, 2005; Lopez et al., 2003; Hemanth, 1999]. Since modeling and simulation of the solidification process imparts an inexpensive prediction methodology for obtaining macro and micro-scale morphology of cast products under varied controlling conditions, the development of such models is of utmost importance for sustainable advancement in this widely deployed manufacturing technology. To understand the physical intricacies and mechanisms associated with a typical casting process involving alloy solidification, a schematic is presented in Figure 1.1 [Bhattacharya, 2014]. Solidification advances from walls towards the interior of the casting domain under consideration due to heat removal from the walls. The system domain is divided into three different regions, namely: (i) fully solid region near the

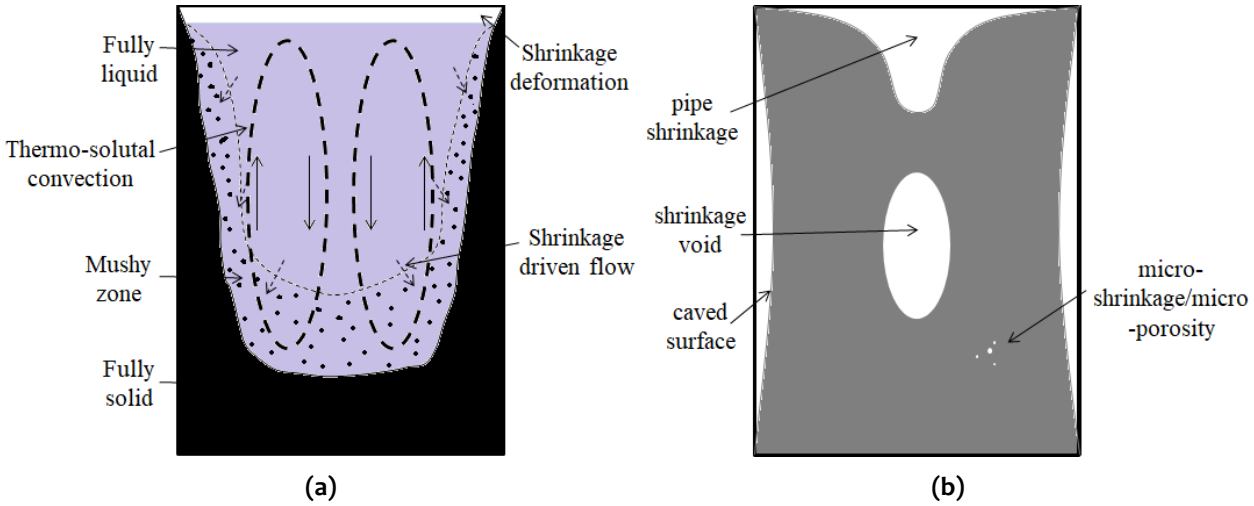

Figure 1.1 : (a) Casting phenomenas observed during solidification, and (b) Final cast structure and defects after complete solidification [Bhattacharya, 2014].

walls, (ii) fully liquid region at the interior core, and, (iii) a mushy region in between the pure solid and pure liquid zone consisting of both solid and liquid phases. A convection current is developed in the pure liquid and mushy regions due to the combined interaction between thermo-solutal buoyancy (double-diffusive) effect and shrinkage effect (Figure 1.1 (a)). The combined effect of shrinkage induced and thermo-solutal convection is manifested by the macro scale surface deformations and presence of macro and micro scale voids entrapped within the final cast product (Figure 1.1 (b)). The micro and macro scale compositional heterogeneities in the cast product are also greatly influenced by the combined effects of the shrinkage and thermo-solutal convection within the melt during the solidification process.

1.1.1 Solidification length scales

Physical attributes that must be taken into account during the model development for the solidification process are defined by the solidification length scale to be addressed by the model. The order of magnitude of the length scale for the solidification process may vary from $1 - 10^{-9}$ m. The lower is the length scale, the better is the resolution of morphological information. However, developing a solidification model that can predict the solidification morphology over the entire range of length scale resolution is neither practical nor attainable, even with the deployment of the most advanced computational facilities available at present. Therefore, models addressing a particular length scale require only a subset of the entire range of physical attributes (describing solidification process for the entire span of the length scale of $1 - 10^{-9}$ m) relevant only to the length scale under consideration. For instance, macro-scale solidification models with length scale ranging from 1 to 10^{-4} m can address the lowest resolution of the order of 10^{-4} m, which is barely sufficient for micro-scale morphological description. Therefore, information obtained from the macroscopic solidification models is bulk average in nature, with all the micro-scale morphological details being represented in a smeared up fashion devoid of any lucid details. A typical example is the macroscopic description of the mushy region. The mushy region consists of both solid and liquid phases. In the macroscopic description, the mushy region is simply described by the volume or mass fraction of solid and liquid phases; and other than this volume/mass fraction based representation of the mushy region, any other morphological details are beyond the scope of such models. On the other hand, a mesoscale solidification model covering a length scale of 10^{-3} to 10^{-5} m is capable of predicting the shape of the solid-liquid interfaces with limited accuracy within primary dendritic arm spacing of the solid crystal structures. Macro-scale physical attributes like thermo-solutal under-cooling and thermo-solutal convection, shrinkage ratio and the bulk porosity of the mushy region play key role in defining macroscopic solidification process. While

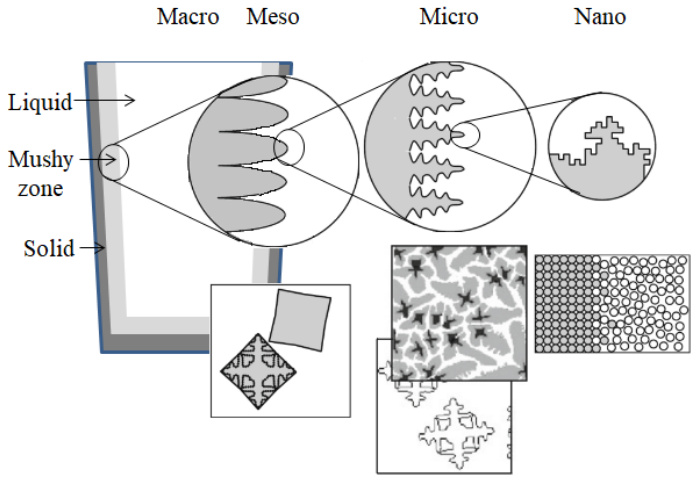

Figure 1.2 : Solidification length scale [Stefanescu, 2015].

some of the physical attributes like anisotropic heat conduction within the solid crystal structure, curvature under-cooling, surface tension play a crucial role in defining mesoscopic description of the solidification process, macroscopic description of solidification does not require these details.

The solidification process at a microscopic level is defined by a length-scale ranging from 10^{-5} to 10^{-7} m. At this length scale, a physical phenomenon like Ostwald ripening due to surface tension is predominant, and the solid-liquid interface can be captured to a resolution of secondary and tertiary dendritic arm spacing. Numerical schemes like phase-field method, level set method, and cellular automata have been successfully deployed to explain the structural behaviour of the solid crystals at mesoscopic and microscopic length scales. At nano-scale ranging from 10^{-8} to 10^{-9} m length-scale, growth and nucleation kinetics of atoms transported from liquid to solid plays the key role in defining the model. Molecular dynamics (MD) simulations are commonly used to capture the solidification morphology at this length scale. A more generic discussion about the time and length scale in solidification science and the adapted numerical methodology is stated in Raabe [1998]. A brief about the same is presented in table 1.1.

The present work focuses on developing macroscopic solidification models with particular emphasis on the shrinkage or volumetric expansion occurring during the solidification process. Therefore, the subsequent discussion is mostly attributed to the macro-scale solidification modeling.

1.2 MACROSCOPIC SOLIDIFICATION AND ASSOCIATED MECHANISMS

The macroscopic description of the solidification process is majorly established on the strong foundation of the conservation principles for mass, momentum, energy, and species dominated by diffusion and advection mechanisms. The most important physical attributes defining the macroscopic solidification models appear as source terms in the governing conservation equations, and they can be described under three broad categories: hydrodynamic, thermal, and solutal (in case alloy solidification is under consideration). The hydrodynamic constraints appear as source terms in momentum conservation equations, while thermal and solutal constraints appear in energy and species conservation equations, respectively [Bennon and Incropera, 1987a,b].

Table 1.1 : Length scales and numerical methodology adapted [Stefanescu, 2015]

Length scale (m)	**Numerical methodology**	**Applications**
10^{-10} to 10^{-6}	Monte Carlo molecular dynamics	Thermodynamics, diffusion, ordering structure and dynamics of lattice defects
10^{-10} to 10^{0}	Cellular automata	Recrystallization, phase transformation, grain solidification and growth, fluid dynamics
10^{-5} to 10^{0}	Large-scale finite element, finite difference, linear iteration, boundary element methods	Averaged solution of differential equations at the macroscopic scale (composition, temperature and electromagnetic fields, hydrodynamics)
10^{-6} to 10^{0}	Finite volume / finite difference method	Solidification, microstructure evolution of alloys, fracture mechanics

1.2.1 Hydrodynamic Attributes

Convection in the liquid melt plays a very crucial role in defining the interface growth and species distribution. In the macroscopic description, alloy systems undergoing solidification can be divided into three distinct domains: pure solid, pure liquid, and mushy region of finite thickness separating two pure phases (Figure 1.2). The mushy region contains both solid and liquid phases with an indistinguishable solid-liquid interface in the macroscopic description. The solid-mushy and mushy-liquid interface evolution during the alloy solidification process depends mostly on the convection current in the melt driven by either naturally occurring thermo-solutal buoyancy effect [Bennon and Incropera, 1987b] or by externally applied force fields in the form of the electromagnetic field [Prescott and Incropera, 1993; Li et al., 2009] and centrifugal force [Riahi, 1997; Fernández et al., 2020]. In the absence of externally applied forces, natural convection driven by thermo-solutal instability in liquid density field defines the flow field within the melt region. The free convection caused by a thermal and solutal gradient in the melt can be immediately identified as the first and most important hydrodynamic attribute to be considered during the solidification process. Density in the liquid phase depends on both temperature and concentration. The change in the density caused by the thermal or solutal variations in the melt produces instability in the buoyancy field. This instability gives rise to convection, known as natural convection. For instance, in a side cooled cavity, the fluid next to the wall is cold and dense as compared to the adjacent bulk liquid. Thus, a force steered by the temperature difference will cause the downward flow of denser and heavier fluid near the wall and a counteracting upward motion of the bulk liquid on the other end of the cavity giving rise to a fluid circulation within the cavity. For alloy systems, once the solidification is initiated, the solute is rejected in the melt adjacent to the solid phase due to the solubility difference between liquid and solid phases. This solute rejection process at the solid-liquid interface causes a solutal gradient to be established in the melt region, giving rise to solutal convection. The direction of flow caused by the solute rejection at the solid-liquid interface depends upon the density of the rejected solute as compared to the solvent. Rejected solute being heavier causes the flow near the interface to be directed in the downward direction, while lighter solute rejection caused upward movement of the melt adjacent to the interface. The combined effect of thermal and solutal gradient gives rise to so-called double-diffusive convection in the melt domain. Depending on the solute-solvent combination, the thermal and solutal buoyancy-driven flows can aid or oppose each other [Hebditch and Hunt, 1974; Ahmad et al., 1998]. The instability of the thermo-solutal buoyancy field is implemented through Boussinesq approximation. In Boussinesq approximation, the density change in the fluid due to thermal or solutal gradient is lumped into source terms like $g\beta_T(T - T_{ref})$ and $g\beta_C(C - C_{ref})$, while the fluid itself is treated as incompressible for the rest of the formulation. Here, g represents gravitational acceleration, β_T,

and β_C are thermal and solutal expansion coefficients, respectively, with the following physical definitions [Stefanescu, 2015].

$$\beta_T = -\frac{1}{\rho}\frac{\partial \rho}{\partial T}\bigg|_C \text{ and } \beta_C = -\frac{1}{\rho}\frac{\partial \rho}{\partial C}\bigg|_T \tag{1.1}$$

The second important hydrodynamic attribute that must be considered during the solidification process is the melt flow within the mushy region. Macroscopic description of the mushy region is simply represented by volume fraction distribution of solid and liquid phases devoid of any morphological information. With the presence of both solid and liquid phases without distinguishable phase interface information in the mushy region, the region can be idealized as a porous medium, where melt can flow through an interconnected porous matrix of the solid phase. Although the existence of the mushy region in the solidifying domain is perfectly valid for alloy solidification, the same is not true when the solidification of a pure substance with fixed freezing temperature is under consideration. The solidification process of a pure substance with fixed freezing or melting point is characterized by the growth of a distinct solid-liquid interface. Does that mean the implementation of porous medium treatment of the mushy zone is invalid for models dealing with such problems? The answer to this question depends on what kind of numerical treatment is implemented to track the solid-liquid interface. If the numerical scheme involves a separate interface tracking scheme that allows adaptive meshing of solid and liquid phases separately, the consideration of the mushy region and the associated porous medium assumption is completely redundant. However, adopting such a scheme is extremely challenging and numerically expensive. Therefore, many solidification models are based on a fixed grid scheme where pure solid and pure liquid regions are separated by a single layer of control volume having solid or liquid volume fraction within the range $0 \leq g_l, g_s \leq 1$ (where, g_l, and g_s are liquid and solid volume fractions respectively, and $g_l + g_s = 1$). The existence of a mushy zone over a single layer of control volumes renders the porosity modeling of the mushy zone inviolable for fixed grid-based solidification modeling of pure substances. Therefore, for fixed gird based solidification models, momentum conservation equations must contain a source term to address the melt flow within the porous mushy region. The source term corresponding to the flow through the porous mushy region often described by Darcy's law defined in the following manner [Bennon and Incropera, 1987a]:

$$F_{i=x,y,z} = \frac{\mu_l}{K_i}\frac{\rho}{\rho_l}(g_l u_i) \tag{1.2}$$

Where, μ_l, g_l, u_i represent dynamic viscosity of the melt, melt volume fraction, melt velocity components in x, y, z directions, respectively, and K_i represents the anisotropic permeability of the porous medium. For simplification the permeability is often treated to be isotropic, *i.e.* $K_i = K$. However, considering varying liquid and solid volume fraction within the mushy region, K is treated to be non-homogeneous, and suitable correlations are used to express permeability K in terms of local solid fraction g_s.

The third important hydrodynamic attribute arises from the fact that solid and liquid phases have different densities causing shrinkage or volumetric expansion effect during the liquid-solid phase transition. During the solidification process, most of the pure metals and metal alloys have a tendency to shrink owing to the higher density of the solid phase. This contraction during solidification can be defined as [Stefanescu, 2015]:

$$\gamma = \frac{\upsilon_l - \upsilon_s}{\upsilon_l} = \frac{\rho_s - \rho_l}{\rho_s} \tag{1.3}$$

Where υ and ρ are specific volume and density, respectively, and subscripts 'l' and 's' represent the liquid and solid phases, respectively. Volume averaging-based macroscopic solidification models use a single set of conservation equations (mass, momentum, energy, and species) for the entire solidification domain. For such models, the shrinkage effect must be reflected in both mass and momentum conservation equations. When we consider the mass conservation equation, in the pure solid and liquid regions, both the phases being treated to be incompressible, the term $\partial\rho/\partial t = 0$ condition prevails in the continuity equation. However, the same can not be stated to be true for the mushy region if the shrinkage effect is under consideration. In the mushy region, liquid and solid phases coexist, and liquid is continuously being transformed into a solid phase. Therefore, shrinkage due to phase transition is predominant in this region and the condition $\partial\rho/\partial t \neq 0$ in the continuity equation must be taken into account. Also, in momentum conservation equations, a source term corresponding to shrinkage appears as a result of the viscous stresses induced by the local density gradients. This particular source term with the mathematical form $\nabla \cdot (\mu_l u_i \nabla(\rho/\rho_l))$ (where, $\rho = g_l\rho_l + g_s\rho_s$, g is volume fraction with subscripts l and s representing solid and liquid phases respectively, and subscript $i = x, y, z$ represents velocity components in x ,y and z directions) play a significant role in defining the shrinkage induced flow [Bennon and Incropera, 1987a; Chiang and Tsai, 1992b].

1.2.2 Thermal Attribute

The latent heat of fusion plays a key role in defining the liquid-solid phase transition. Depending on the modeling scheme, the term associated with the latent heat of fusion may appear in the governing equations in a different manner. For instance, solidification models involving separate governing equations for solid and liquid phases, the moving solid-liquid interface represents the common boundary between the two phases, and energy balance at the interface provides the means to track the interface growth. The equation involving energy balance at the interface is known as Stefan Equation [Dantzig and Rappaz, 2016]. Stefan equation equates heat removal rate at the solid side of the interface with the combined effect of latent heat removal rate required for the solid front growth and the sensible cooling rate at the liquid side of the interface. Therefore, in models involving separate energy conservation equations for separate phases in the domain, the term associated with the latent heat is reflected through the latent heat removal rate required for the solid front growth in the Stefan equation. On the other hand, volume averaging based models use a single energy conservation equation for all the phases present in the domain. In such models, the interface is also part of the solution domain and a natural outcome of the solution procedure. Therefore, the term/terms involving latent heat appears/appear in the energy conservation equation itself [Voller and Prakash, 1987]. However, the tracking of the interface in volume averaging based models requires the evaluation of an extra parameter namely; mass fraction (f_l = mass fraction of liquid and f_s = mass fraction of solid satisfying the condition $f_l + f_s = 1$) or volume fraction (g_l = volume fraction of liquid and g_s = volume fraction of solid satisfying the condition $g_l + g_s = 1$) of liquid and solid phases at individual control volumes. For the solidification of pure substances with distinct freezing or melting point, the interface is defined by a single layer of control volume satisfying the condition $0 \leq g_l, g_s \leq 1$, separating the region of pure solid phase defined by $g_l = 0$ and the region of pure liquid phase having $g_l = 1$ [Brent et al., 1988]. On the other hand, the solidification of alloys involves three regions of finite thicknesses, namely pure solid region ($g_l = 0$), mushy region ($0 < g_l, g_s < 1$), and pure liquid region ($g_l = 1$) [Voller and Prakash, 1987]. When the volume averaging scheme is implemented to derive a single energy conservation equation valid for the entire solidification domain, the energy equation is often described in terms of temperature T as the primary scalar variable. In such representation of energy conservation equation, the source term/terms involving latent heat of fusion (h_{sl}) always appear with a multiplication factor of g_l along with other multiplication or division factors involving density and specific heat. The combined representation of $g_l h_{sl}$ particularly manifests an extremely important physical significance. $g_l = 1$ and $g_l = 0$ values render this term to become equal to h_{sl}

and 0 respectively, designating pure liquid phase to have an excess enthalpy of h_{sl} as compared to the pure solid phase at the melting/freezing point. The solidification of alloys is a more complex phenomenon if the alloy under consideration has a non-eutectic composition. Solidification of the non-eutectic alloy being characterized by phase change over a temperature range rather than at a distinct temperature; solidification ensues only after the local temperature attains a value less than liquidus temperature (T_L) corresponding to the local composition of the liquid phase. The variation of the local composition of the liquid phase depends on the solubility difference between the liquid and solid phases and the species advection process. Therefore, modeling of a non-eutectic binary alloy solidification also involves solving a species conservation equation. In fact, solidification of an n^{th} order alloy system containing n components in it requires $(n-1)$ species conservation equations to be solved along with continuity, momentum, and energy conservation equations.

We often encounter a large difference between specific heats of liquid and solid phases for most pure substances and alloy systems [Chakraborty, 2017]. In fact, in the majority of the cases, the specific heat of the liquid phase is higher than that of the solid phase. Many of the existing mathematical models deal with this problem by considering a constant average specific heat value for both the phases. However, a more realistic model involves consideration of different specific heat values for solid and liquid phases. Representation of the volume-averaged energy conservation equation with T as the primary scalar variable along with the consideration of different specific heats for solid and liquid phases gives rise to two more source terms in the form of advection flux term and transient term, respectively.

It is pertinent to mention here that in the absence of a separate interface tracing formulation, evaluation of g_l or g_s is crucial to determine the interface. However, the solution of the governing conservation equations, namely mass, momentum, energy, and species (required for non-eutectic alloy solidification models only), provide the solutions for pressure, velocity, energy, and species compositions only. Therefore, evaluation of g_l or g_s needs one extra formulation scheme. One of the most popular scheme to attain this particular formulation to evaluate g_l or g_s is through using a numerical artifact, commonly known as enthalpy updating scheme or volume fraction updating scheme [Voller and Prakash, 1987; Brent et al., 1988; Chakraborty, 2017]. The implementation of the enthalpy updating (volume fraction updating) method to obtain g_l or g_s, along with the porous medium treatment of the mushy region, corresponds to the name of this well-known solidification modeling scheme as enthalpy porosity method.

1.2.3 Solutal Attribute

Numerical modeling of alloy solidification process involves solving species conservation equation/equations along with mass, momentum, and energy conservation equations. For a binary alloy system, a single species conservation equation serves the purpose. However, for higher-order alloy systems, the species conservation equation must be solved for each of the additional components [Bennon and Incropera, 1987a; Diao and Tsai, 1993; Chen and Tsai, 1993]. For alloy solidification modeling, the source terms in the species conservation equation arise from the fact that solid and liquid phases have different solubility. The solubility in the solid and liquid phases at a given temperature lying between liquidus and solidus temperatures can be obtained from the temperature-composition diagram or phase diagram of the alloy system under consideration. A representative phase diagram is shown in figure 3. The solubility of the solid phase being lesser than that of the liquid phase, the species concentration in the liquid phase (C_l) and solid phase (C_s) are related by the relation: $C_s = k_p C_l$, in a representative control volume undergoing solidification process. The parameter k_p is called the partition coefficient, and k_p is always less than unity as long as liquid phase species concentration (C_l) is less than eutectic composition (C_e). When $C_l = C_e$, k_p becomes unity, designating $C_l = C_s = C_e$. Treating k_p to be constant corresponds to the assumption that liquidus and solidus temperature lines are considered

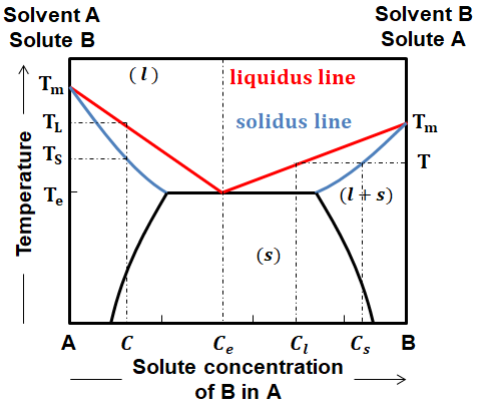

Figure 1.3 : Binary alloy phase diagram.

to be linearly proportional to the species concentration in the phase diagram representation of the alloy system.

For control volumes undergoing solidification process, the condition $0 < g_l, g_s < 1$ prevails. As a result, solid and liquid phases coexist in those control volumes. However, owing to the low solubility of the evolving solid phase, solute gets rejected in the liquid phase within those control volumes leading to a local enrichment of the species concentration in the liquid phase. The diffusion and advection of this solute rich melt from the control volumes undergoing solidification process to the surrounding control volumes give rise to diffusion and advection based source terms in the species conservation equation. Since liquidus temperature (T_L) is defined by the local liquid concentration and the formulation pertaining to the evaluation of g_l or g_s is strongly dependent on T_L, estimation of g_l is inherently coupled with the estimation of local C_l values. In volume averaging models species concentration in a control volume is defined by $C = f_l C_l + f_s C_s$, with C being the primary scalar variable. From the estimated value of C at a control volume undergoing the solidification process, C_l is derived using the lever rule or Scheil model. The basic assumption of the lever rule considers infinite species diffusion within solid and liquid phases within the control volume length scale and C_l is estimated using the formulation $C = C_l(f_l + k_p f_s)$, with the estimation constraint $C_l = C_e$ in case we obtain $C_l > C_e$. On the other hand, the basic assumption of the Scheil model is infinite species diffusion in the liquid phase and zero diffusion in the solid phase within the control volume length scale. For Scheil model C_l is estimated using the formula $C = f_l C_l + k_p(f_s - f_s^0)C_l + f_s^0 C_s^0$, where, f_s^0 and C_s^0 represents mass fraction and species concentration in the solid phase at the previous time step. Once again, C_l is set to C_e, if $C_l > C_e$. It is pertinent to mention here that assumptions corresponding to lever rule or Schiel model is only restricted within the control volumes undergoing the phase transformation and should not be mixed up with the macro-scale species diffusion coefficients D_l or D_s, which are rather small ($\sim 10^{-9}$ to $10^{-11} m^2 s^{-1}$) in magnitude [Stefanescu, 2015].

1.3 IMPORTANT OUTCOMES FROM MACROSCOPIC SOLIDIFICATION MODELING

Next, we discuss the expected outcomes of the solidification models. Other than predicting the velocity, temperature, species concentration (valid for alloy systems only) evolution during the solidification process, the macroscopic solidification model is beneficial to furnish information regarding the nature of the interface growth, macro-defects related to shrinkage, and most importantly, the macro-segregation or the compositional inhomogeneity of the final cast product

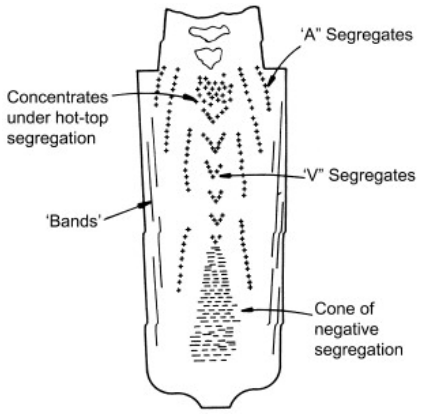

Figure 1.4 : Distribution of macrosegregation after complete solidification of an ingot [Stefanescu, 2015].

when alloy solidification process is involved. Macro-segregation, being directly related to the mechanical properties of the final cast product, is well worth special research attention. All these outcomes have a strong dependence on the cooling rate, cooling orientation, and initial conditions. The predictions of macroscopic casting defects obtained from the simulations being invaluable inputs for improving the casting products, we focus on the two most important outcomes of these models: macro-shrinkage defects and macro-segregation.

1.3.1 Macro-shrinkage Defects

When a material, be it a pure substance or an alloy, is undergoing the solidification process within a confinement or mold, shrinkage or volumetric expansion is inevitable due to the difference between liquid and solid phase densities. Other than very few substances like water and silicon manifesting volumetric expansion during liquid to the solid phase transition, most materials undergo volumetric contraction or shrinkage during the solidification process. While volumetric expansion might cause undesirable residual stresses within the final cast product, the defects associated with shrinkage is more severe in nature, and the shrinkage induced defects are manifested by the formation of macro and micro voids in the final cast products. The shrinkage defects can be avoided by ensuring a continuous supply of molten metal to the growing solid front to compensate for the shrinkage effect associated with the solidification process. In the absence of such provision to feed the liquid metal continuously to the growing solid front results in shrinkage defects in the cast products. Figure 1.1 (b) shows the typical shrinkage defects encountered during the solidification process. As is evident from Figure 1.1 (b), shrinkage induced defects can be manifested by external surface deformation of the cast product as well as by the existence of internal micro or macro voids. Macro or micro voids are often caused by the entrapped dissolved gases in the melt. Surface deformation is typically caused by the shrinkage induced flow, while macro and micro voids are controlled by the combined effects of pore nucleation cites and shrinkage induced flow. For conventional casting methods, risers and runners are added to the mold cavity in order to avoid shrinkage induced macro-voids within the mold region. Inappropriate cooling orientation and cooling rate mostly contribute to the formation of shrinkage defects in the cast products leading to a large number of rejections during mass-scale production. Thus, the development of solidification models capable of predicting shrinkage defects is of utmost importance for obtaining reliable optimal cooling orientations and cooling rates to minimize shrinkage defects in casting. The precise projection of shrinkage defects can be obtained by implementing a suitable volume averaging scheme applied for the simultaneous existence of solid, liquid, and gaseous phases in a representative control volume and solving for the coupled governing equations: mass, momentum, energy, and species conservation equations.

1.3.2 Macrosegregation

Macro-segregation corresponds to the spatial inhomogeneity of composition encountered during the metal alloy solidification process. The length-scale of macro-segregation may range from $10^3 - 1$ m depending on the size of the cast products [Stefanescu, 2015]. Such inhomogeneity in composition distribution has an undesirable impact on the material properties of the cast products and subsequent material processing, leading to a large number of rejections of the as-cast components. In fact, macro-segregation is an inherent attribute for any alloy solidification process, be it the mass-scale production of steel ingots or precision growth of semiconductor crystals. Particularly for cast products with a large length scale, the severity of macro-segregation needs to be attenuated during the casting process itself. The complete mitigation of macro-segregation after the completion of the casting process cannot be attained by further heat treatment processes due to the low diffusivity of solute in the solid phase and the requirement of achieving solutal homogeneity over a large length scale.

Macro-segregation primarily results from the solubility difference in liquid and solid phases and the flow of liquid and solid phases adjacent to the solid-liquid interface. Most of the alloy systems are characterized by a solid phase with much lower solubility than the liquid phase. A typical binary alloy phase diagram shown in Figure 1.3 manifests this solubility difference in liquid and solid phases. Liquid-solid phase transition causes the rejection of excess solute in the liquid phase adjacent to the newly transformed solid phase. As a result, the melt adjacent to the growing solid front becomes rich in solute, while the primary solid contains lower solute concentration. The length scale of solutal segregation due to the difference in phase solubility is restricted to the length scale of microstructure, typically defined by the primary dendritic arm spacing having an order of magnitude ranging between $10^{-5} - 10^{-4}$ m. Such segregation of species being restricted within the microstructural formation is called micro-segregation. However, melt flow caused by natural mechanisms like shrinkage or thermo-solutal buoyancy results in transportation and redistribution of highly segregated liquid near the solid front to the neighboring melt regions. Since the effect of melt advection is felt over a much larger length scale, the redistribution of solute through the melt flow gives rise to macro-segregation in cast products. The combined effect of solute rejection and solute advection during the alloy solidification process gives rise to a distribution of positive and negative macro-segregation within the cast product, where positive and negative segregations correspond to the solute concentrations above and below the nominal alloy composition, respectively. It is pertinent to mention here that the average species concentration over the entire casting domain must be equal to the nominal concentration following the species conservation principle. Methods pertaining to the prevention of macro-segregation include the imposition of density stratification through adjusting the thermal and solutal gradients, controlling of cooling rate, inoculation, electromagnetic stirring, inert gas impingement, and many more. In the absence of an external mechanism, gravity or buoyancy driven flow plays the most significant role in defining the macro-segregation in the cast product. Figure 1.4 shows some of the typical macro-segregation patterns found in the as-cast ingots like V-type, A-type, and conical segregation patterns [Stefanescu, 2015]. The major outcome of macroscopic solidification model is the prediction of the macro-segregation pattern under the influence of varying cooling orientations and cooling rates.

1.4 OBJECTIVES

With the above-stated preamble, we proceed to define the objectives of the present thesis. It is clear from the above discussion that at different solidification length scales, a different set of physical attributes become more relevant over others. For the macro-scale definition of the solidification process, in particular, thermo-solutal advection and shrinkage are undoubtedly the two most important physical attributes that define macroscopic defects and macro-segregation

in a cast product. Thus, a thorough understanding of these two phenomena and their mutual interaction is essential to improve the quality of cast products. Although the influence of thermo-solutal advection on the solidification process is extensively studied both experimentally and numerically, macroscopic solidification model development addressing shrinkage effect rarely received much research attention. Therefore, the principal objective of the present work is to develop macroscopic solidification models inclusive of shrinkage effect at different capacities to study and explore the influence of shrinkage on various important process outcomes like interface growth rate, macro-segregation, and macroscopic defects pertaining to surface deformation and void formation. Solidification models addressing the shrinkage effect are developed in the following order. In the first two chapters, one-dimensional diffusion based semi-analytical models are developed for solidification of pure substance in a finite domain, where shrinkage effect is incorporated through implementing mass conservation in the domain. While the first chapter deals with model development pertaining to the prediction of solid front growth for a given cold temperature boundary condition, in the second chapter, a semi-analytical scheme is proposed to solve the inverse problem concerning the prediction of the cooling curve for prescribed interface growth rate. In the next two chapters, multi-dimensional solidification models associated with shrinkage induced flow is developed for pure substance and binary alloy systems. The final chapter deals with multi-dimensional solidification model development involving free surface tracking to capture shrinkage induced defects during the solidification of binary alloy systems. All the models proposed in this work are validated with the experimental and theoretical data either available in existing literature or obtained from an in-house experimental facility. A more detailed scope of this thesis is discussed in the concluding section of the present introductory chapter.

1.5 REVIEW OF LITERATURE

In the past few decades, a significant amount of research has been conducted to comprehend the theory of the solidification process. The analytical and numerical models for both macro-scale and micro-scale is developed to analyze various phenomena during solidification. Most of these theoretical studies are accompanied by experimental investigations for validation. In the present section, a detailed state of the art review is provided that corresponds directly to the outline of this thesis. To start with, the literature associated with analytical models of directional solidification of metals and non-metals are reviewed, followed by literature dealing with the numerical models involving shrinkage induced flow during solidification of metals and alloy systems. Special emphasis is also attributed to those solidification models pertaining to the prediction of shrinkage defects and macro-segregation. In the concluding section of the chapter, gaps and opportunities particularly related to the inclusion of the shrinkage effect in existing solidification models are identified to formulate the scope of this thesis.

1.5.1 Analytical macro-scale modeling of solidification shrinkage

A great many physical attributes associated with the interface movement and grain growth during the solidification process can be addressed by physically consistent analytical models. Some of the close form solutions to diffusion dominated Stefan's solidification problem are presented by Worster [1986], Ozisik [2002] and Rappaz and Dantzig [2009]. Worster [1986] in his work derived an analytical solution for a one-dimensional alloy solidification problem. During the analysis, the growth of mushy-layer within a semi-infinite domain was studied for an aqueous salt solution. Rappaz and Dantzig [2009] reported an analytical model for solidification of pure substance in a mold; however, the model involves similar semi-infinite consideration for the liquid domain. Chakraborty and Dutta [2003] employed an analytical model involving quasi-steady state with semi-infinite consideration while studying cyclic melting and freezing of phase change materials (PCM) used for thermal management of electronic devices. Recently, Natale et al. [2010] proposed

an explicit analytical scheme for solving one-dimensional free boundary problems involving solidification process considering shrinkage and volumetric expansion. Once again, the solution involves semi-infinite formulation for the liquid phase, and the report, although discussed the theory, is devoid of any case study. Since the analytical model involving shrinkage or volumetric expansion within a finite domain has rarely been reported [Natale et al., 2010], it is well worth some research effort to develop such models.

Directional grain or crystal growth has many applications in the areas related to the production of high-frequency turbine blades, solar absorber materials, photovoltaic materials, and many more. Crystal growth is a fundamental phenomenon, defining the grain structure during solidification processes. Favorable mechanical properties such as strength and hardness of cast products can be achieved by controlling grain structure [Hemanth, 1999; Lopez et al., 2003; Gokhale and Patel, 2005]. Attempts have been made to refine the microstructure of castings by adding refiner and modifier to the melt to improve the mechanical strength of cast products [Liao et al., 2002]. One of the most important factors that influence the growth of micro-structure is the cooling rate (K/s) [Boettinger et al., 1984; Sarreal and Abbaschian, 1986; Zhuang and Langer, 1989; Zhang et al., 2000; Taha et al., 2002; Eskin et al., 2005; Du and Jacot, 2005; Du et al., 2007; Zhang et al., 2008; Kasperovich et al., 2008; Hosseini et al., 2013]. Boettinger et al. [1984] reported the prevalence of conventional dendritic or eutectic structures at low crystal growth rate condition and suggested the possibility of obtaining micro-segregation-free single-phase structures at higher crystal growth rates. Sarreal and Abbaschian [1986] and Taha et al. [2002] reported the existence of an optimal cooling rate for achieving the maximum amount of non-equilibrium eutectic (NEE) phase in the directionally solidified sample of non-eutectic alloys. Sarreal and Abbaschian [1986] and Taha et al. [2002] interpreted this phenomenon as a result of back diffusion, dendrite tip under-cooling, and eutectic temperature depression. Zhuang and Langer [1989] in his work, achieved a fine equiaxed grain structure of Co-Cr-Mo alloys by employing a fast cooling rate during the casting process. As an effect of controlled boundary, the interdendritic coarse patchy carbide structure was substituted by a grain boundary of fine particles. Eskin et al. [2005] performed a set of controlled casting experiments on an Al-Cu binary alloy system with different cooling rates (0-10 K/s) and casting condition. It was inferred that the fraction of non-equilibrium eutectic has a high dependence on cooling rate in a disproportionate form. To interpret the experimental observation of Eskin et al. [2005], Du et al. [2007] developed a 2-D segregation model that employs pseudo-front tracking (PET) method to analyse the solidification and grain structure. Zhang et al. [2008] studied the influence of the fast cooling method by using a copper mold for solidification of Al356 alloy. Similarly, Hosseini et al. [2013] studied the effect of cooling rate on mechanical properties, solidification parameters, and micro-structures of LM13 alloy. Zhang et al. [2008] and Hosseini et al. [2013] concluded that higher cooling rate and shorter solidification time causes further refinement of micro-structures, resulting in segregation-free micro-structures with a homogeneous distribution of micro-porosity. Kasperovich et al. [2008] investigated non-eutectic Al-Cu alloy solidification under the influence of a large range of cooling rates (0.01-20000 K/s) to conclude a similar trend. Kasperovich et al. [2008] also used a 2-D PFT model developed by Du and Jacot [2005] to predict the eutectic fractions and validated the numerical results with experimental data.

Uncontrolled cooling rate causes the inhomogeneous distribution of grain-size and micro-porosity, which may lead to severe casting defects [Zhang et al., 2008; Hosseini et al., 2013]. Challenge of determining an appropriate cooling curve to ensure the desired crystal growth rate received considerable attention from several research groups [Dorschu, 1968; Mullin and Nỳvlt, 1971; Lukens et al., 1981; Alkemper et al., 1998; Gandin, 2000b,a]. The experimental investigation reported by Dorschu [1968] involves controlling the cooling rate during the gas metal arc welding process. Since the experimental procedure to find the cooling rate is expensive, Mullin and Nỳvlt [1971] proposed a programmed cooling mode by developing a mathematical model to predict cooling curves based on data measured during the crystallization process of aqueous

potassium and ammonium sulfate system. It was observed that the preliminary cooling rate of the conducive cooling curve is relatively steady, whereas the cooling rate is substantially stiff at the extremity of the cooling curve. Restricted experiments on cooling rate control with the help of surface temperature sensing devices were reported by [Lukens et al., 1981], where the cooling rate of the weld metal was monitored by means of infrared technique in order to study micro-structures near the weld bead. Alkemper et al. [1998] described an experimental study involving uni-directional solidification of Al-Si alloy under controlled solidification parameters like velocity and temperature gradient of the melt. Gandin [2000b,a] described a 1-D heat flow model to study uni-directional solidification of pure Al and Al-Si alloy. Gandin [2000b,a] determined the interface velocity using experimentally obtained cooling curves incorporating the effect of shrinkage. From all these literature reviews, it is evident that grain growth is one of the key parameters deciding the morphology of microstructure, and cooling rate is one of the most important controlling parameters that define the grain growth. Therefore, prior knowledge of the cooling curve can be extremely beneficial to obtain a desired crystal growth rate. Determining the cooling curve for the desired growth rate analytically or numerically is not a straightforward problem and involves an inverse solution technique. The literature review reveals the absence of suitable theoretical models for predicting the cooling curve, and an effort towards developing such models might be of extreme relevance to the crystal growth applications.

1.5.2 Numerical macro-scale modeling of solidification shrinkage

In this subsection on the literature review, we focus, particularly on existing multi-dimensional solidification models. Phase change mechanism associated with solidification and melting is an intrinsic component of manufacturing processes like casting and welding, and thermal management applications involving latent heat thermal energy storage, cyclic cooling of electronic equipment, and many more. The physics associated with the solidification process is multi-scale in nature, spanning from nano to macro scale. State of the art manufacturing technologies like additive manufacturing processes involving laser sintering, laser surface alloying essentially deal with melting and re-solidification mechanisms. Numerous complex flow physics involving Marangoni convection due to surface tension [Dutta et al., 1995; Sarkar et al., 2002; Raj et al., 2002; Kashchiev, 2003], natural convection, shrinkage convection [Zhang and Faghri, 1999; Chen and Zhang, 2006; Xiao and Zhang, 2006] play a key role in defining the desirable mechanical properties of the products manufactured through such advanced processes. Thus, understanding the flow physics in the context of the solidification process is of utmost importance to achieve improved product yield at an industrial scale. The broad area of contemporary and advanced manufacturing applications involving the melting and solidification process instigated commendable research work by several research groups over the past few decades.

Regardless of clarity in definition, the physics associated with the solidification process is complex to perceive. The foremost concern related to the solidification process is to track the evolving solid-liquid interface. There exist three different classes of the solidification process, namely, (a) distinct, (b) alloy, and (c) continuous. The distinct solidification process involves the existence of a sharp interface between solid and liquid phases, typically featuring solidification of pure metals. Alloy solidification process involves regions of columnar and equiaxed crystalline structures with complex shapes of solid-liquid interface and typically encountered during the solidification of metal alloys. For the continuous solidification process, the individual phases are dispersed in every part of the phase change region, and no distinct interface exists. Typical examples of the continuous solidification process are the freezing of oil, wax, and polymers. Distinct interface tracking can be achieved by well established front tracking method [Unverdi and Tryggvason, 1992; Tryggvason et al., 2001; De Sousa et al., 2004], level set method [Sussman et al., 1998], and marker and cell method [Harlow and Welch, 1965]. However, for alloy and continuous solidification processes interface is hardly distinct, and the tracking methods are computationally

expensive and difficult to implement [Voller et al., 1990]. One of the reliable schemes to address all three types of solidification processes is the fixed grid-based enthalpy or volume fraction updating method. The major advantage of fixed grid enthalpy updating method [Voller et al., 1990] is the redundancy of explicit coupling requirements for energy and mass balance at the interface location. Several researchers have reported a considerable number of numerical models involving well-established enthalpy updating scheme to solve pure metal or binary alloy solidification [Voller et al., 1987; Voller and Prakash, 1987; Brent et al., 1988; Swaminathan and Voller, 1992, 1993; Chakraborty, 2017].

The enthalpy updating formulation for capturing solid-liquid interface during solidification of pure metals and binary alloys was originally proposed by Voller et al. [1987]; Voller and Prakash [1987]. The key feature of the above formulation is the inclusion of local variation of latent heat of fusion as a source term in the energy conservation equation and the iterative evolution of the same. Brent et al. [1988] proposed a farther modification of the above model and reported that a faster convergence is possibly obtained for the solidification under the effect of natural convection by using the enthalpy porosity approach. Recently, Chakraborty [2017] proposed a modified enthalpy updating method that evaluates solid or liquid volume fraction and simulates phase change process for materials with a substantial difference between phase-specific heats.

All the proposed solidification models involving enthalpy updating scheme till date have the limitation of considering the same density of liquid and solid phases. Shrinkage or volumetric expansion effects due to the difference between liquid and solid phases is an important aspect of the solidification process for most of the pure substances and alloys. The incorporation of the effects of different phase densities within the present framework of the enthalpy updating scheme will lead to a more reliable numerical scheme to predict the evolution of all three types of solidification processes. The existing solidification models that involve shrinkage effect are rarely found in the literature [Xu and Li, 1991; Chiang and Tsai, 1992b,a; Krane and Incropera, 1995]. Among the few existing models involving the shrinkage effect, the pioneering model was proposed by Chiang and Tsai [1992b,a]. The analysis reported by Chiang and Tsai [1992b,a] involves directional solidification from the bottom side of 1 % Cr-Steel in a rectangular cavity with a riser at the center. This particular configuration was chosen to suppress all other possibilities of natural convection. Unlike side cooling and top cooling orientation [Xu and Li, 1991; Krane and Incropera, 1995; Satbhai et al., 2019], cooling from the bottom ensures the existence of stably stratified thermal buoyancy field, leading to complete suppression of thermal buoyancy-driven free convection. The bottom cooling configuration was chosen by Chiang and Tsai [1992b] to ensure that the advection in the melt during the solidification process is driven by shrinkage effect only. However, the absence of source term associated with natural convection in the analysis reported by Chiang and Tsai [1992b] nullified any possibility of interaction between the buoyancy and shrinkage induced source terms from the modeling point of view. The possibility of such interaction needs to be explored further. Since the macro-scale flow mechanism during the solidification process is dominated by both thermo-solutal buoyancy effect and shrinkage effect, the interaction between these two mechanisms defines the melt-flow pattern and macro-segregation in the final cast product. Therefore, the inclusion of shrinkage induced flow aspect in the solidification model is crucial for obtaining realistic prediction of macro-scale casting defects involving surface deformation, internal voids, and compositional inhomogeneity [Flemings, 1974; Fisher, 1981].

The next set of the literature review concerns the binary alloy solidification process in the presence and absence of shrinkage induced flow. During directional solidification of an alloy system in a bottom cooled cavity, the thermal gradient along the vertically upward direction is positive with a stably stratified thermal buoyancy field. However, depending on the relative heaviness or lightness of the solute with respect to the solvent, the solutal expansion coefficient

needs to be assigned with negative or positive values. If the rejected solute to the melt during the alloy solidification process is heavier than the solvent, the solutal expansion coefficient is negative, indicating overall volume reduction of solute enriched melt leading to stable stratification of solutal buoyancy field and reinforcement of the already existing stably stratified thermal buoyancy field. On the other hand, rejection of lighter solute in the melt during alloy solidification process assigns a positive solutal expansion coefficient, indicating an overall volume expansion of the solute enriched melt promoting instability of the solutal buoyancy field and formation of plumes.

The development of the mushy region is caused by the solute rejection phenomena occurring during the phase transformation process [Flemings, 1974; Worster, 1986, 1991, 1992; Worster and Kerr, 1994; Stefanescu, 2015; Dantzig and Rappaz, 2016]. During solidification, the melt near the solid phase becomes rich in solute concentration, causing depression of liquidus temperature. As a result, the liquid-solid phase transition process is deferred till the local temperature attains this lower liquidus temperature value. The region beyond solute rich melt being solute lean, the corresponding higher liquidus temperature in this region promotes initiation of liquid-solid phase transition. However, the region closer to the cold wall is still undergoing the solidification process with coexisting liquid and solid phases. As a result, the alloy solidification process is characterized by the existence and growth of a mushy layer of finite thickness where solid and liquid phases coexist. The region adjacent to the cold boundary being the coldest region, complete solidification is eventually attained as the local temperature approaches the eutectic temperature of the alloy system. Thus, the solidifying domain during the alloy solidification process consists of pure solid and liquid regions separated by a mushy layer of finite thickness. The mushy layer is characterized by a steep gradient of solute concentration due to the solute rejection mechanism associated with the liquid-solid phase transition. From the hydrodynamic point of view, rejection of lighter solute during the alloy solidification process is more interesting since the rejection of lighter solute promotes solutal instability in the trapped melt inside the mushy layer. Depending on the strength of this instability, the effect can be farther propagated to the pure liquid region leading to the melt convection within and beyond the mushy region [Sarazin and Hellawell, 1988; Felicelli et al., 1991; Jamgotchian et al., 2004]. The melt convection plays a key role in defining the mushy layer growth, and macro-segregation in the final cast product is of direct consequence of the mushy zone growth mechanism. Therefore, it is extremely important to study the effect of solutal instability on the evolution of the mushy region.

Inverse segregation encountered due to the heavier solute rejection in the melt during solidification of the binary alloy has been studied and explained by several researchers ([Diao and Tsai, 1993; Chen and Tsai, 1993; Gao et al., 2017, 2019]). Similarly, channel formation in the mushy region due to lighter solute rejection in the melt during the directional solidification of metal alloys ([Sarazin and Hellawell, 1988; Felicelli et al., 1991; Bergman et al., 1997]) or inorganic alloys ([Chen and Chen, 1991; Emms and Fowler, 1994; Chen et al., 1994; Chen, 1995]) is a well-studied subject area for many decades. Simulations considering shrinkage induced flow performed by Diao and Tsai [1993]; Chen and Tsai [1993] successfully predicted the inverse segregation during the bottom-up solidification of Al-Cu alloy, and validation was made with the published experimental results of Kato and Cahoon [1985]. In a more recent work by Gao et al. [2017], a mathematical model is developed on the basis of redistribution behavior to predict the micro-segregation and porosity during Al-Cu alloy solidification. The study shows the porosity effect within the mushy zone, causing the suppression of segregation phenomena. However, the formulation is devoid of any energy advection terms, rendering the energy transfer to be diffusion dominated. The above work is farther improved by Gao et al. [2019] to consider the mass variation in the mushy region. Here, the effect of inter-dendritic flow is incorporated and is applied to predict porosity and inverse segregation during uni-directional solidification of Al-Cu alloys.

Next, we present some of the literature reviews concerning lighter solute rejection and

associated freckling phenomena during the directional alloy solidification process in bottom cooled orientation. Felicelli et al. [1991] in his work presented a mathematical model that simulates the freckle formation. Importance was given to the initiation of freckles and the conditions affecting the nucleation of freckles. Worster [1991] provided an analytical solution to the equations that drive the growth of the mushy region by incorporating the effects of solutal buoyancy-driven convection. Instability analyses have also been carried out by Worster [1992] for uni-directional solidification of binary alloys within the mushy and liquid zone. Two systems of solutal buoyancy field were investigated by employing a linear stability analysis: 'mushy layer mode' directed within the porous medium of the domain, and 'boundary layer mode' directed within the meta-stable liquid region adjacent to the mushy-liquid interface. Emphasis was given to the mushy layer mode of instability. A study was also performed to determine the inception of the mushy layer during bottom-up solidification of an alloy due to interaction between solutal convection and undercooling at the mushy-liquid interface [Worster and Kerr, 1994]. The effect of contamination on the onset of solutal instability was investigated in detail by adding a small amount of $CuSO_4$ into the aqueous solution of ammonium chloride. Chiareli et al. [1994] and Chiareli and Worster [1995] considered the effect of a density difference between fluid and solid, in the absence of solutal buoyancy effect and analysed the mushy layer instability with the conclusion that the instability can occur only in the case of expansion. Numerical models proposed by Schulze and Worster [1998]; Chung and Worster [2002] were distinctly focused on obtaining steady-state solutions for the problems with specified channel positions. However, these models do not address the cause and onset of channel formation, neither do they analyse the flow interaction between the adjacent channels. Katz and Worster [2008] proposed a 2-D numerical model based on Darcy's law and the enthalpy method to avert imposing explicit conditions on the solid-mush-liquid interfaces. The analysis was performed using NH_4Cl-H_2O solution, and the results obtained were compared with the experimental data presented by Peppin et al. [2008]. Chakraborty and Dutta [2013] numerically modeled the freckle formation during bottom-up solidification of NH_4Cl-H_2O solution. The detachment of solid particles and advection of solid particles along with the melt was observed experimentally and implemented numerically. However, the shrinkage effect was unaccounted for during the solidification process. In addition to double diffusion during directional solidification, Anderson and Worster [1996] studied an oscillatory instability within the mushy region, which was later modified for ternary alloy system by Guba and Anderson [2014].

Shrinkage effect has been considered to model inverse segregation associated with heavier solute rejection in the melt during directional solidification binary alloy involving bottom cooling orientation[Diao and Tsai, 1993; Chen and Tsai, 1993]. However, studies involving the effect of shrinkage induced flow on freckle formation caused by lighter solute rejection in the melt during the solidification process of the binary alloy is rarely reported [Sajja and Felicelli, 2011]. Challenges associated with the modeling of freckling phenomena during directional solidification of the binary alloy due to rejection of lighter solute in the melt is much more formidable when additional complexities involving the inclusion of shrinkage induced flow is accounted for. Therefore, modeling of channel formation in the mushy region and associated macro-segregation arising from the coupled interaction between shrinkage induced and solutal convection poses a very interesting problem statement.

Minimizing casting defects like porosity, shrinkage cavity, and macro-segregation is of utmost importance to ensure the quality of the final cast products. However, the prediction of these defects using numerical models is very complex. The modeling complexities arise from the fact that the presence of all three phases, namely solid, liquid, and gas, along with their interactions at phase interfaces, needs to be addressed in such models. Although experimental studies associated with shrinkage defects can provide substantial information related to casting control parameters, suitable solidification models capable of predicting shrinkage defects can contribute in this regard in a much more inexpensive fashion. Incremental efforts are made to predict the evolution of

surface defects during the solidification process by many research groups [Chiang and Tsai, 1992b; Bounds et al., 2000; Wang et al., 2005; Raessi and Mostaghimi, 2005; Sun and Garimella, 2007; Ge et al., 2017; Chen and Shen, 2019; Niu et al., 2019]. Among the existing literature, Bounds et al. [2000] studied the macro-defect by solving coupled free surface, momentum, and energy equation. The scheme to solve the convection equation was intricate with convergence issues. Wang et al. [2005] analyzed a three-phase volume averaging model to study globular equiaxed solidification following the free surface deformation. Also, pressure variation close to the free surface with and without consideration of grain growth was examined. Further, the result of density variation within solid and liquid has been carried out by Raessi and Mostaghimi [2005], which predicted the macro-scale open shrinkage cavity. A general 3-D formulation was followed, and the shape of the shrinkage cavity was captured using the VOF method [Nichols et al., 1980]. The numerical model developed was based on 2-D Eulerian code RIPPLE [Kothe et al., 1991], which was mainly designed to solve free surface flows incorporating surface tension effect. Furthermore, numerical and experimental investigations were performed by Sun and Garimella [2007] to study solidification shrinkage and by Ge et al. [2017] to study macro-segregation with shrinkage. Chen and Shen [2019] developed an arbitrary Lagrangian-Eulerian (ALE) model to anticipate macro-segregation owing to shrinkage and thermal-solutal convection during alloy solidification. Niu et al. [2019] in their work used a smooth particle hydrodynamics method to predict the shrinkage cavity. All the above existing models reveal a strong dependence of the shrinkage-defect shape on the heat removal rate. None of these existing predictions involves an enthalpy updating scheme to evaluate solid and liquid volume fractions [Voller and Prakash, 1987; Chakraborty, 2017]. Thus, it is very important to find the validity of the enthalpy updating scheme regarding the prediction surface deformation due to shrinkage by the inclusion of density difference between solid and liquid phases in the existing framework of the scheme.

1.5.3 Experimental investigation of directional solidification

Experiments involving directional solidification with bottom cooling configuration are performed to study macro-segregation [Kato and Cahoon, 1985; Rerko et al., 2003; Ferreira et al., 2004, 2009], grain growth [Ziv and Weinberg, 1989; Alkemper et al., 1998; Gandin, 2000a], and convection owing to density anomaly of fluid [Sarazin and Hellawell, 1988; Chen and Chen, 1991; Chen, 1995; Jamgotchian et al., 2004; Kumar et al., 2017, 2018c,a, 2019]. At the macro-level, experiments were generally performed using aluminium cast alloys; and the formation of pipe shrinkage or internal shrinkage cavities were studied by observing sections of the cast product [Evans et al., 1992; Bounds et al., 2000; Reis et al., 2012]. Chen and Chen [1991] performed experiments using aqueous solution of ammonium chloride for different bottom cooled temperature, varying from -31.5 ^oC to 11.9 ^oC. The channel formation was observed within the mushy region for the temperature as high as 11 ^oC; however, a further increase in cold boundary temperature at the bottom ceased the plume formation. The mush porosity was determined using the tomography technique. Chen [1995] presented results for different experimental techniques used to obtain a better understanding of convection occurring within the mushy zone. Different sets of experimental designs were proposed by employing (i) dye tracing method: to study convection before and after the onset, (ii) hele-shaw 2-D cell: to have a thorough view of convection within chimneys, and (iii) using X-ray tomography: to determine the porosity within the mushy region. The effect of different experimental configurations on convective and morphological instabilities was described by Jamgotchian et al. [2004]. Different crucible diameters were chosen, and experiments were performed using succinonitrile-acetone and lead-thallium alloys. Recently, an experimental investigation was also carried out by Kumar et al. [2018a] to address the effect of solutal composition over freckle formation for NH_4Cl-H_2O binary solution, where the composition was measured using Mach-Zehnder interferometry. The study was further extended to investigate the role of mushy zone permeability in driving the buoyancy flow patterns in faceted and dendritic growth during bottom-up solidification of KNO_3-H_2O and NH_4Cl-H_2O

binary solution respectively [Kumar et al., 2020]. The results showed a peculiar behaviour of decreasing and sudden increase in temperature during solidification for KNO_3 aqueous solution as compared to a monotonous decrease in temperature for NH_4Cl-H_2O solution. To the best knowledge of the present authors, no experimental study addressed shrinkage induced flow and its effect on solid front growth till date during directional solidification. In the end, the summary of the literature is drawn up specifically addressing the shrinkage associated work. The scope and limitations are mentioned within the table 1.2.

Table 1.2 : Summary of literature addressing shrinkage

Literature	**Approach**	**Study / Limitations**
Worster [1986]	Analytical	Performed analysis for 1-D semi-infinite domain. Limitation(s): Semi-infinite solution would not be applicable to finite domain. Material: water, $NaNO_3$ + H_2O
Rappaz and Dantzig [2009]	Analytical	Performed analysis for 1-D semi-infinite domain. Limitation(s): Semi-infinite solution would not be applicable to finite domain. Material: Fe-C
Natale et al. [2010]	Analytical	Performed shrinkage/volumetric expansion analysis for 1-D finite domain. Limitation(s): The solution involves semi-infinite formulation in solid and liquid domain. No validation. Material: No examples
Mullin and Nỳvlt [1971]	Mathematical	Developed data based mathematical model to predict cooling curve. Limitation(s): No shrinkage Material: potassium and ammonium sulphate system
Alkemper et al. [1998]	Experiment	Studied uni-directional solidification for alloy system under controlled solidification parameters (velocity and temperature gradient). Material: Al-Si alloy system
Gandin [2000b,a]	Analytical/ Experiment	Developed 1-D heat flow model to study directional solidification of alloy system. Determined interface velocity using experimentally obtained cooling curves incorporating shrinkage. Limitation(s): Crude methodology. No convectional analytical approach used. Material: Al-Si alloy
Voller et al. [1987] Voller and Prakash [1987]	Numerical	Proposed enthalpy updating formulation for capturing solid-liquid interface during alloy solidification. Limitation(s): Densities were assumed to be same within phases.

Continued on next page

Table 1.2 – continued from previous page

Literature	Approach	Study / Limitations
		Material: Pseudo material
Brent et al. [1988]	Numerical	Modified above model to gain faster convergence using enthalpy porosity technique. Limitation(s): Similar phase density case. Material: Pure Gallium
Chakraborty [2017]	Numerical	Proposed modified enthalpy updating method to evaluate volume fraction for large phase specific heats. Limitation(s): Similar phase density case. Material: Water
Xu and Li [1991] Krane and Incropera [1995] Chiang and Tsai [1992b]	Numerical	Studied (shrinkage + body force term), for side cooling case. Limitation(s): Volume averaged enthalpy updating. Material: Al-4.5wt.%Cu; Pb-19.2wt.%Sn; 1%Cr-steel
Chiang and Tsai [1992b,a]	Numerical	Studied shrinkage effect for bottom cooling orientation. Limitation(s): Neglected the body force term. Devoid of interaction between shrinkage and body force term. Material: 1% Cr-steel
Kato and Cahoon [1985]	Experiment	Performed directional solidification experiments to study inverse segregation for Al-Cu alloys. Limitation(s): No evidence showcasing the negative segregation in mushy region. Material: Al-4.1wt.% Cu
Diao and Tsai [1993] Chen and Tsai [1993]	Numerical	Studied inverse segregation for bottom cooled configuration. Limitation(s): No enthalpy updating scheme. Material: Al-4.1wt.% Cu
Gao et al. [2017, 2019]	Numerical	Studied porosity effect within the mushy zone, causing the suppression of segregation phenomena. Limitation(s): Formulation is devoid of energy advection terms. Material: Al-4.5wt.% Cu
Sajja and Felicelli [2011]	Numerical	Studied the freckle formation caused by lighter solute rejection in the melt in presence of shrinkage. Limitation(s): No numerical and experimental validation. Material: Pb-23 wt. % Sn
Sun and Garimella [2007]	Numerical/ experiment	Performed numerical analysis using Ansys-Fluent to capture shrinkage cavity. Limitation(s): Enthalpy updating

Continued on next page

Table 1.2 – continued from previous page

Literature	Approach	Study / Limitations
		methodology should be examined. Material: Trinitrotoluene (TNT)
Ge et al. [2017]	Numerical	Performed numerical analysis to study macro-segregation and formation of shrinkage cavity. Methodology: Phase field formulation. Material: Fe-3.3 wt. % C

1.6 SCOPE OF THE THESIS

From the literature review, it is evident that there exists an appreciable opportunity and need for solidification model development addressing the inclusion of the shrinkage effect. Development of solidification model addressing the effect of shrinkage on convection, inverse segregation, channel formation, free surface deformation during solidification of pure substances or alloys is extremely challenging owing to the involvement of multi-physics at various length scales. An analytical model pertaining to uni-directional solidification in the finite domain in the presence of shrinkage is yet to be found in the existing literature and needs to be developed. The effect of shrinkage induced convection during directional eutectic/alloy solidification needs some rigorous investigation and experimental evidence for thorough understanding. In addition, the formation of shrinkage defects such as free surface deformation along with associated macro-segregation is also needed to be analysed. In view of these gaps, the following five chapters are organised in a systematic manner to address various attributes of shrinkage during solidification process. A brief description of the contents of the five subsequent chapters are provided as follows:

1. **Chapter 2:** The content of this chapter involves the development of a 1-D semi-analytical solidification model for pure substance involving shrinkage effect. Analytical models involving density change during the solidification process has hardly acquired any attention [Natale et al., 2010]. To investigate shrinkage or volume expansion, a semi-analytical model is developed for a finite domain. The solid-liquid interface movement is tracked by solving the energy conservation (Stefan's equation) at the interface, while the free surface movement is addressed by considering the overall conservation of mass for the solidifying domain. The analytical solution obtained from the proposed model is validated with the existing enthalpy updating based numerical model [Voller et al., 1987; Brent et al., 1988; Chakraborty, 2017], considering water as a solidifying fluid. Once validated, case studies are performed considering water and paraffin as phase change material to study the volumetric expansion and shrinkage effects, respectively.

2. **Chapter 3:** In this chapter, an inverse solidification model is proposed to predict the cooling curve for prescribed unidirectional crystal growth rate associated with the solidification of pure substances or alloys with eutectic composition. The controlled cooling rate is associated with a homogeneous distribution of grains and microstructure that prevents casting defects [Zhang et al., 2008; Hosseini et al., 2013]. However, the prediction of an appropriate cooling curve involving shrinkage effect is rarely attempted. The study in this chapter aims at developing a reliable inverse solidification model to determine required temperature evolution in time at the cold boundary to obtain a desired interface growth rate during the solidification of pure substance or eutectic alloys restricted within a finite length scale.

3. **Chapter 4:** A fixed grid-based numerical modeling scheme to address shrinkage induced macroscopic flow during the solidification of a pure substance is developed and validated with experimental observations in this chapter. As is evident from the literature review, the enthalpy updating scheme is successfully implemented for simulating solidification problems. Even though the scheme is simple and efficient, to date, it has not been implemented with the involvement of the shrinkage effect. In this chapter, an attempt has been made to improve the existing enthalpy updating scheme by incorporating the shrinkage effect. However, the evolution of the free surface is not addressed in this chapter, and a continuous supply of melt at the inlet cavity in the form of a riser opening is considered. In a previous numerical study by Chiang and Tsai [1992b], for bottom cooling orientation, the effect of buoyancy force was neglected. In this mold chapter, an investigation is performed to study the interaction between shrinkage induced source term and buoyancy source term and their combined effect on solid front growth during the distinct and continuous solidification processes associated with the liquid-solid phase transition of pure substance. The model is validated by performing a set of controlled experiments to obtain velocity field and interface growth using particle image velocimetry technique during the solidification of coconut oil.

4. **Chapter 5:** In this chapter, the model developed in the previous (4^{th}) chapter is extended further to study the effect of shrinkage flow on directional binary alloy solidification with bottom cooled orientation. Although the inverse segregation phenomena associated with heavier solute rejection during the directional binary alloy solidification is reported in the literature, studies involving the effect of shrinkage induced flow in conjunction with lighter solute rejection and associated freckle formation is rarely reported [Sajja and Felicelli, 2011]. Therefore, modeling of channel formation in the mushy region and associated macro-segregation arising from the coupled interaction between shrinkage induced and thermo-solutal convection is investigated in this chapter. Since experimental results involving the influence of shrinkage induced flow on freckle formation is nonexistent to the best knowledge of the author, the model validation is obtained only with the existing results concerning inverse segregation involving heavier solute rejection the solidification of binary alloys [Diao and Tsai, 1993; Chen and Tsai, 1993; Kato and Cahoon, 1985].

5. **Chapter 6:** This chapter is attributed to the model development to predict shrinkage defect in the form of free surface deformation during binary alloy solidification. The effect of shrinkage flow on the free surface deformation is accounted for by using the volume of fluid method during the alloy solidification process. The existing models reported in the literature reveals a strong dependence of the shape of shrinkage-defects on the heat removal rate. None of these existing predictions involve an enthalpy updating scheme to evaluate solid and liquid volume fractions. The present study focuses on modifying the enthalpy updating scheme in its existing framework to include tracking of the evolving free surface caused by shrinkage induced flow. The results of the numerical model is compared with the existing numerical and experimental results reported by Sun and Garimella [2007].

6. **Chapter 7:** In this chapter, comprehensive conclusions concerning all the key findings of the constitutive chapters, 2-6 of the thesis are presented. A grand overview of the thesis and the future research scope are also highlighted in this chapter.

…